How To Concentrate an Aqueous Polyelectrolyte/Surfactant Mixture by Adding Water

Philippe Ilekti,[†,‡] Lennart Piculell,*[,†] Florence Tournilhac,[‡] and Bernard Cabane[‡]

Physical Chemistry 1, Center for Chemistry and Chemical Engineering, Lund University, Box 124, S-221 00 Lund, Sweden, and Equipe mixte CEA-RP, Rhône-Poulenc, 93308 Aubervilliers, France

Received: August 7, 1997; In Final Form: November 11, 1997[⊗]

Aqueous systems containing sodium polyacrylate (NaPA) and the surfactant cetyltrimethylammonium bromide (CTABr) can separate into a concentrated phase and a dilute phase. The phase separation can be induced by addition of water. Further addition of water causes the concentrated phase to become still more concentrated. A structural analysis of the concentrated phase shows that the surfactant ions (CTA^+) are always aggregated into elongated micelles. These micelles are packed with short-range order (concentrated micellar phase) or long-range order (hexagonal phase). The ionic compositions of the concentrated and the dilute phase have been determined. They indicate that the association results from an ion-exchange process, where the polyacrylate ions displace some bromide counterions of the surfactant aggregates. The separation of a dilute aqueous phase and the deswelling of the concentrated phase are then explained by the gain in entropy of the simple salt (Na^+ and Br^-) that is released in the dilute phase.

Introduction

The mixing of a dilute aqueous solution of an ionic surfactant with a dilute solution of an oppositely charged polymer generally results in a phase separation whereby a concentrated phase is formed that is enriched in both the charged polymer and the surfactant. This phenomenon is well documented,[1] and its analogy with the phase separation in mixtures of two oppositely charged polymers has been recognized.[2] In the polymer/surfactant case, it is the surfactant *aggregate*, formed by hydrophobic self-association of the surfactant molecules, that plays the role of one of the charged polymers. Nevertheless, the concentrated phases that separate have generally been insufficiently characterized with respect to both their detailed composition and their structure. There are reports on both isotropic phases and mesophases,[3] but it has not been clear how—or, indeed, why—these structures depend on the overall compositions of the mixtures. An interesting question also concerns the relation between these structures and the sequences of structures found in the binary surfactant/water mixtures at different compositions. Moreover, there is a gap to be bridged between phase studies on the one hand and studies of hydrated complex salts, formed by surfactant ions with polyions as their only counterions, on the other. The latter salts are void of the small inorganic counterions that normally accompany the surfactant ion and the charged polymer, and they have been found to form interesting mesophases[4−6] or vesicles[7,8] under more or less hydrated conditions.

An important step in the understanding of oppositely charged polymer/surfactant mixtures was taken by Thalberg et al.[9−13] They realized that a complete description of the phase behavior of such mixtures is only possible in terms of five components: water and the four different neutral salts that may be obtained by combining the four ionic species in the mixture. To provide the necessary background to our study, we will digress a moment to discuss some of the implications of this fact. We will then also need to define a terminology to be used throughout this paper to describe the four ionic species in the mixtures and their corresponding pure salts: (1) The *surfactant* is the salt formed by the *surfactant ion* together with its (normal) *simple surfactant counterion*; (2) The *polyelectrolyte* is the salt composed by the polymeric *polyion* and its *simple polyelectrolyte counterion*; (3) The *simple salt* is the salt formed by the two oppositely charged simple ions; (4) The *complex salt* is the salt formed by the surfactant ion and the polyion.

Thalberg et al. showed that the full phase diagram could be represented in three dimensions by a tetragonal pyramid, with water at the top and with the four neutral salts at the apexes of its quadratic base (Figure 1). This is in contrast to the *conventional phase map* shown in Figure 2a. The latter diagram, which has been used in some previous studies,[3,14] shows the appearance of systems obtained by mixing polyelectrolyte, surfactant, and water in various proportions. The total compositions of these mixtures thus represent a plane in the full phase diagram (Figure 1), which we will call the *conventional mixing plane* containing all possible mixtures of the polyelectrolyte, surfactant, and water. The typical feature of the conventional phase map is a droplet-shaped area close to the water corner, representing total compositions where phase separation is observed. This area is surrounded by a single-phase area representing compositions that do not demix. The problem with this map is that it cannot be used to describe the compositions of the phases in phase-separated samples. This is because, as shown by Thalberg et al., these compositions are not at all situated in the conventional mixing plane. When attempts are nevertheless made to project these compositions onto the mixing plane, they lead to seemingly confusing results: The concentrated equilibrium phases are not situated on the boundary of the one-phase region in the phase map, but they are typically much more concentrated.[3,14]

An alternative approach to these mixtures would seem to be more revealing. Since the system contains two ions that have a strong tendency to separate out together as the complex salt,

* Author for correspondence.
[†] Lund University.
[‡] Rhône-Poulenc.
[⊗] Abstract published in *Advance ACS Abstracts,* December 15, 1997.

S1089-5647(97)02575-3 CCC: $15.00
Published on Web 01/08/1998

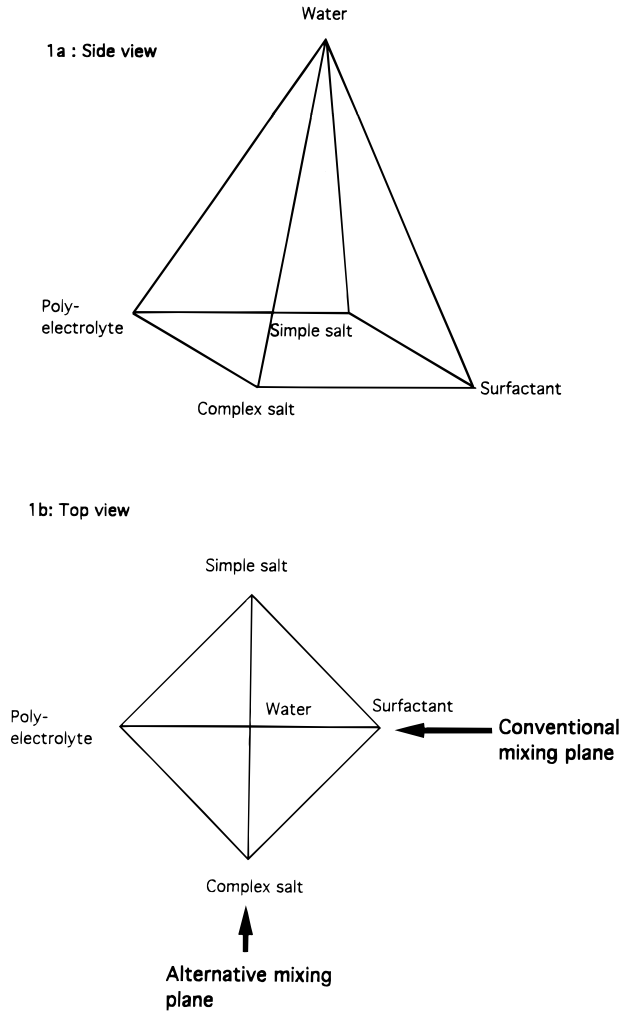

Figure 1. Pyramidal phase diagram: side view (a) and top view (b).

and two other ions that basically stay in solution as the simple salt, it should be more natural to attempt a description in terms of this *alternative mixing plane* by generating a phase map of mixtures of complex salt, simple salt, and water. Figure 2b shows the expected features of such a diagram for a hypothetical perfectly symmetric case, where the complex salt is formed by two identical polyions that differ only by the signs of their charges. The complex salt is quite insoluble in pure water (hence, the miscibility gap on the right axis), but as more and more simple salt is added (along line 1 in the diagram), the electrostatic attractions between the oppositely charged polyions become progressively more screened. This results in a swelling of the concentrated phase and in the development of a finite solubility of the complex salt in the dilute phase. Finally, at sufficient amounts of added simple salt, a one-phase area is reached.

For the perfectly symmetric system in Figure 2b, the separating phases generated in the alternative mixing plane must (because of the symmetry) indeed lie on the boundary of the one-phase area. Therefore, we have indicated tielines in the diagram. These illustrate what is expected to happen if water is added to a concentrated monophasic mixture (along line 2 in the diagram). The system should eventually phase-separate, and as more and more water is added, the concentrated phase, enriched in the complex salt, should become more and more concentrated. This is because the system becomes more and more dilute in the simple salt; hence, the screening effect is progressively weakened, and the effective attractions between

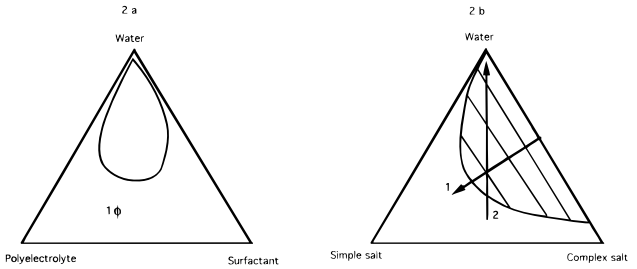

Figure 2. Schematic phase maps describing the phase separation in the conventional mixing plane (a) and in the alternative mixing plane (b).

the polyions become progressively stronger. Note that the latter effect should be general for any complex salt, independent of the symmetry assumed in Figure 2b. This thought experiment (which we will verify by our experiment below) illustrates the expected dependence of the phase behavior on the total water content, which is not at all obvious from the normal phase map in Figure 2a. This is because the content of simple salt is a hidden variable in the latter diagram.

The objective of this work is then a first attempt to describe in a satisfactory way how the phase diagram of an oppositely charged polyelectrolyte/surfactant/water mixture varies with the overall water content. What are the compositions of all the ionic species in the separating phases? What structure(s) do we find in the concentrated phases that separate out? For simplicity, and for illustrative purposes, we have focused our efforts on samples with stoichiometric compositions (equal numbers of charges of all ionic species) and where the only variable is the amount of water. This set of samples forms a particularly instructive series, since their overall composition belong to both mixing planes described above. They may equally correctly be described as stoichiometric mixtures of polyelectrolyte and surfactant *or* of complex salt and simple salt.

We emphasize the fact that our objective with this work has been to obtain complete data on the compositions, as well as information on the structures, of the separating phases. Despite the vast amount of work that has been performed already, this type of data is not available from previous studies. What is particularly missing is data on individual ionic species. We have therefore chosen to study a simple system where the concentrations of all ionic species in each of separating phases could be determined. The surfactant was cetyltrimethylammonium bromide (CTABr). Because of the long alkyl chain length (16 carbons), the hydrophobic interactions between surfactant molecules are quite strong, and all surfactant molecules are aggregated. The polyelectrolyte was sodium polyacrylate (NaPA). Because of the high charge density of polyacrylate, its interaction with the surfactant aggregates is also quite strong. The molar mass of the polyion was low (Mw = 2000 g/mol), which made it possible to prepare samples at high polyelectrolyte concentrations. Finally, this system has a high contrast in X-ray scattering, which made it possible to determine the structures of all phases.

Materials and Methods

Materials. Poly(acrylic acid) (Mw = 2 000 g/mol) was purchased from Aldrich. Sodium polyacrylate was obtained by addition of an equivalent amount of sodium hydroxide to ionize the acid functions of the polymer. The pH of the sodium polyacrylate solutions was about 8. Consequently, all the carboxylic function were ionized. Solutions of this polyelec-

trolyte in 0.1 M $LiNO_3$ were examined through size-exclusion chromatography (SEC) coupled with low-angle light scattering (LALS). It was found that the polyelectrolytes had a number average molar mass $M_n = 2800$ g/mol and a weight average mass $M_w = 4700$ g/mol. The polyelectrolyte concentration is expressed in weight percent (%) of monomer or in mole of monomer per liter. CTABr was purchased from Merck and used without further purification.

Methods. We focused on stoichiometric samples where the charge ratio between the polyion and the surfactant was always equal to 1. All samples were initially prepared in the monophasic region at high concentration (18.5% surfactant and 4.8% polyelectrolyte). Then the samples were diluted with Millipore water to obtain the points at lower concentration. The samples were heated to 50 °C and centrifuged at 25 °C for 10 h at 3000 rpm to obtain a complete separation of phases. They were then stored at 25 °C. Both phases were separated and carefully weighed.

Elemental analyses were performed on each of the separating phases.

(1) In the dilute phase, the sodium and the bromide ions were analyzed by capillary ion analysis (CIA), the polyion was analyzed by carbon analysis and with SEC, and the surfactant ion was analyzed by a colorimetric titration. It is a two-phase titration method using sodium dodecyl sulfate as titrant, a mixture of cationic indicator (dimidium bromide) and an anionic indicator (Sulphan Blue), and chloroform as the organic phase. We verified that the presence of the polyion had no effect on the result on this titration within a 5% error margin.

(2) The concentrated phase was solubilized in water at low pH with nitric acid. The surfactant ion was analyzed with the same colorimetric method. The concentrations of sodium and bromide ions were determined by CIA.

No analyses were made on the three-phase samples because of the difficulties of isolating each phase.

The polyion and water contents in the concentrated phase were calculated from the sodium, surfactant ion, and bromide analyses using the electroneutrality of the concentrated phase and from the total weight of the concentrated phase. The carbon analysis made on the dilute phase and the dried content of the concentrated phase support these calculations. Then, from the initial quantities, the amount left in the dilute phase was calculated.

Small-angle X-ray scattering measurements were performed on a Kratky compact small-angle system with a linear collimation. The X-rays were detected with a position-sensitive detector. The sample-to-detector distance was 277 mm and the wavelength 1.54 Å.

Results

Phase Separation. A conventional phase map of the regions of phase separation in the system (water, NaPA, CTABr) at 25 °C is shown in Figure 3. The main feature is the phase-separation region located next to the water corner. For compositions in this region, the polyelectrolyte/surfactant mixtures phase-separate. For compositions outside this region, the system forms a single-fluid phase.

From now on, we focus on samples with compositions on the stoichiometric line (the straight line in Figure 3) where the charge ratio between the polyelectrolyte and the surfactant equals unity. A linear map of the phase behavior of these samples is presented in Figure 4. The samples were initially prepared within the single-phase region at high concentration, I_{conc} (right-hand side). This single phase is fluid and transparent. Samples

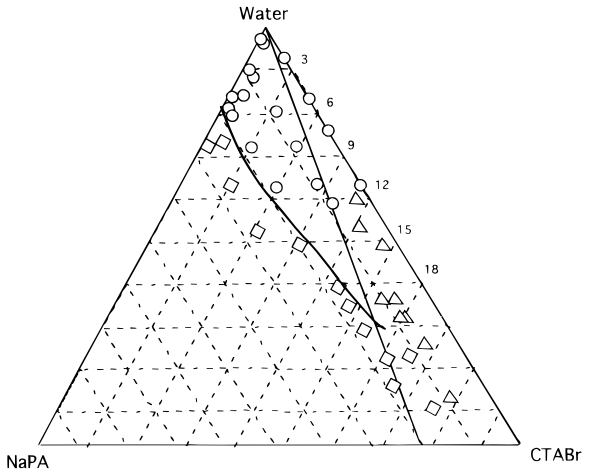

Figure 3. Conventional phase map of NaPA with CTABr in water at 25 °C indicating monophasic samples (squares), phase-separated samples (circles), and samples where the CTABr crystallized (triangles). The weight concentration (%) of the CTABr is indicated along the water−CTABr axis. The straight line corresponds to charge stoichiometry.

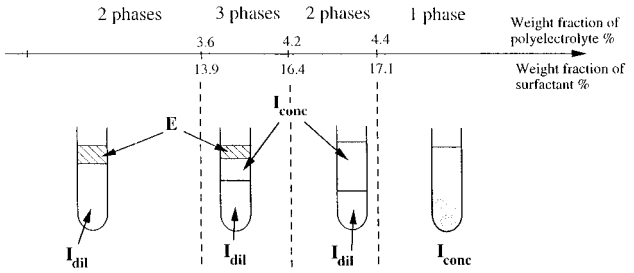

Figure 4. Linear phase map along the stoichiometric line. The horizontal scale indicates the initial compositions of the samples before phase separation.

of lower overall concentration were made by addition of water to this phase. When the surfactant concentration was brought below 17.1%, another transparent phase, I_{dil}, separated out at the bottom. This phase was heavier and less viscous than I_{conc}, and it contained less surfactant and polyelectrolyte. When the addition of water brought the surfactant concentration below 16.5%, a third phase, E, separated out on the top of the samples. This phase was a turbid paste. Further addition of water caused the concentrated phase I_{conc} to vanish when the surfactant concentration was lowered below 13.9%. As more water was added to the two-phase system that remained, the turbid paste became whiter and harder.

After visual observation of the phase separation, the phases were removed for structural determination and composition analysis.

Structures. Observation through optical microscopy with crossed polarizers indicated that the fluid phases were isotropic, while the turbid paste was birefringent. Accordingly, we expect the fluid phases to be micellar and the turbid paste to be a mesophase.

SAXS spectra of the concentrated phases are shown in Figure 5. The spectrum of the viscous transparent phase (I_{conc}; Figure 5a) only shows a broad peak, similar to the peak caused by the interferences between neighboring micelles in pure CTABr solutions. Therefore, this phase also has a micellar organization.

The spectrum of the turbid paste from a sample with an initial surfactant concentration of 13.2% is shown in Figure 5b. Two sharp peaks can be seen; the first one is much more intense, and the ratio of their q values is 1.73, which matches that for

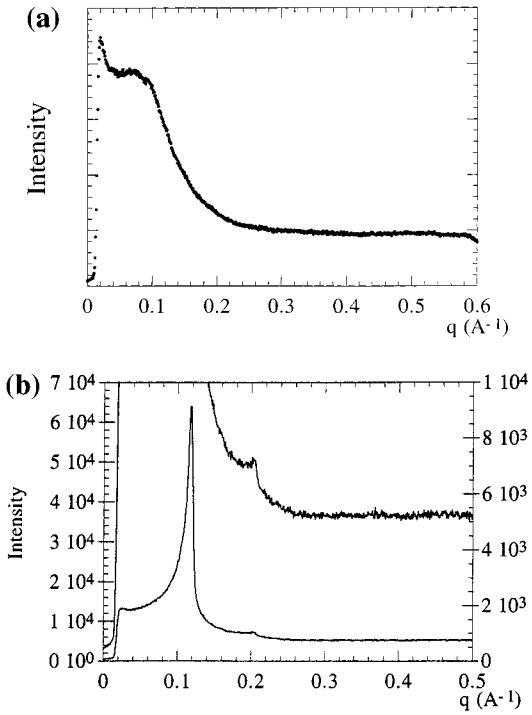

Figure 5. X-ray spectra of a monophasic sample prepared with 18.3% surfactant and 4.8% polymer (a) and of the concentrated phase of a two-phase sample prepared with 13.2% surfactant and 3.4% polymer (b).

a hexagonal organization made of cylindrical objects. The positions of both peaks shifted to higher q (shorter distances) when more water was added, indicating that the cylinders were pushed closer together. Measurements of the dried weight of the concentrated phase indicated that the total concentration of surfactant and polyelectrolyte (55%) had increased. From this, we concluded that the cylinders were surfactant aggregates and that water was between them; i.e., the phase E was a normal hexagonal phase, similar in structure to the hexagonal phase of the pure surfactant.

At very large additions of water, a lamellar structure was obtained instead of the hexagonal structure. Other phases were also found at nonstoichiometric compositions. These results will be reported in a later publication.

In summary, the addition of increasing amounts of water to the samples caused the separation of a dilute phase I_{dil} from the initial isotropic-concentrated phase I_{conc}. With addition of more water, the I_{conc} phase became more and more concentrated and, eventually, an even more concentrated hexagonal phase, E, separated out. On addition of still more water, the I_{conc} phase disappeared and the E phase became increasingly more concentrated.

Composition. The counterintuitive behavior described immediately above was confirmed by systematic measurements of the dried weight of the concentrated phases and of the carbon content of the dilute phases. These results are presented in Figure 6. As before, we describe them starting from the single-phase region I_{conc} at high overall concentration (right-hand side).

In the first two-phase region (initial solid content below 21.7%, surfactant concentration below 17.1% in Figure 4), the top phase of the sample had a total concentration slightly above that of the preceding single phase while the lower phase of the sample was much more dilute. This is why both the top phase and the original single phase are denoted as I_{conc}.

In the second two-phase region (initial solid content below 17.5%, surfactant concentration below 13.9% in Figure 4), the top phase of the sample had a still higher concentration, rising from 45 to 51% as more water was added. This was the hexagonal phase, denoted E in the previous section. The bottom fluid phase started at the same concentration as the I_{dil} phase. For this reason it was also labeled I_{dil}. It became still more depleted in surfactant and polyelectrolyte as more water was added.

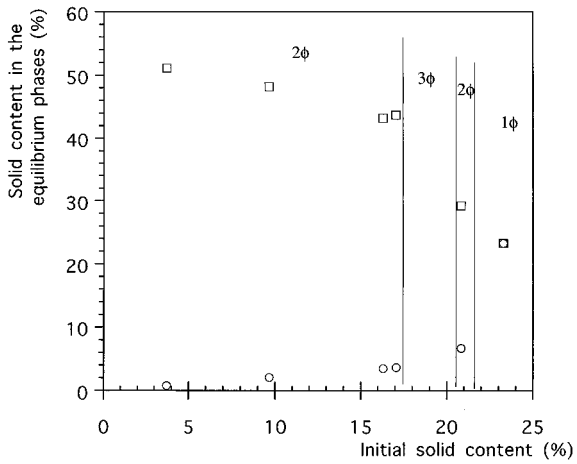

Figure 6. Solid content (%) of the dilute (circles) and concentrated (squares) phases as functions of the initial content (%) of solids (polymer + surfactant/polymer + surfactant + water) in the samples before phase separation.

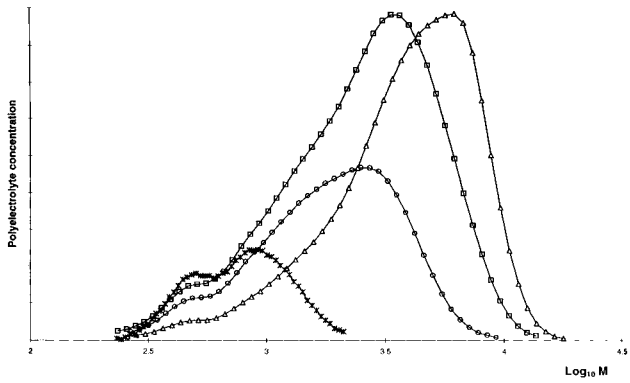

Figure 7. Concentration of the polyelectrolyte versus polyelectrolyte molecular weight for a 0.11% NaPA solution (triangles) and for dilute phases of biphasic samples prepared with 12.9% surfactant and 3.3% polyelectrolyte (squares), 7.6% surfactant and 2% polymer (circles), and 1% surfactant and 0.26% polymer (crosses).

Altogether, Figure 6 confirms that the addition of water causes the separation of concentrated phases that hold less and less water from a dilute phase that becomes still more dilute.

It was also of interest to determine which were the ions that were released in the dilute I_{dil} phase as it formed. Colorimetric titration indicated that the surfactant ion concentration in this phase was quite low (lower than 3%). Therefore, the carbon content of the dilute I_{dil} phase originated from the polyions. As more water was added to the two-phase samples, this amount of polyion was also reduced to almost zero.

Since the polyion was not monodisperse, it was of interest to investigate the molecular-weight distributions of the polyions in the concentrated and the dilute phases. For this purpose, the dilute phase I_{dil}, which contained no surfactant, was examined by SEC. The results are shown in Figure 7. Starting from the right-hand side, the first trace corresponds to a solution of NaPA (0.11%) alone in water; it shows a broad main peak and a very small subsidiary peak corresponding to oligomers. The next trace (squares) corresponds to the I_{dil} phase that

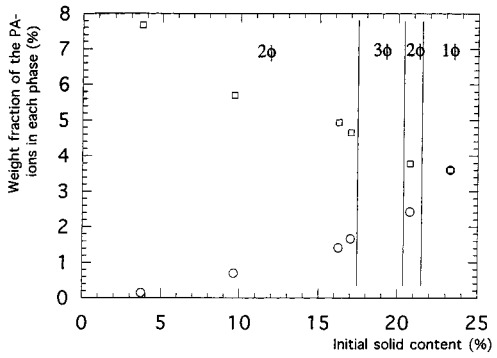

Figure 8. Weight fraction of PA^- ions in each phase versus the initial solid content.

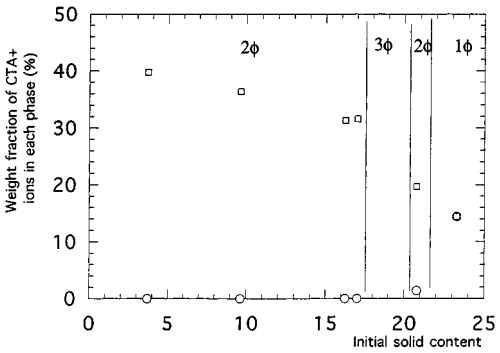

Figure 9. Weight fraction of CTA^+ ions in each phase versus the initial solid content.

separated when the surfactant concentration was 12.9%. The peak has the same shape as the one for the pure NaPA solution, but it is slightly shifted toward lower molecular weight, indicating that the phase-separation process produces some fractionation of the polyions. The two other traces correspond to I_{dil} phases that separated out when more water was added. For the lowest one, the main peak has vanished, indicating that all large polyions had gone to the concentrated phase. Thus, addition of water to the two-phase samples caused the dilute phase to be progressively depleted in the polyions. These variations are shown in Figure 8.

The distribution of all other ions in the separating phases are shown in Figures 9−11. They show a number of remarkable features.

(1) The surfactant ions were almost totally absent in the dilute I_{dil} phase, that is, all of them remained in the concentrated phases I_{conc} and/or E. As more water was added to the two-phase samples, these concentrated phases became more concentrated, and therefore, the surfactant ion concentration rose (i.e., going from the right to the left in Figure 9)

(2) The bromide ions were also unevenly distributed among the separating phases, but the distribution changed with the addition of water. For low amounts of water (right-hand side of the E phase in Figure 10) the distribution of bromide resembles that of the surfactant ions; most of the Br^- ions are with the CTA^+ ions in the concentrated phase (top) and few of them in the dilute phase (bottom phase). This distribution became less uneven when more water was added. Obviously, Br^- ions were lost to the large volume of the dilute phase, while PA^- ions were transferred to the concentrated phase (compare Figure 8).

(3) Sodium ions were evenly distributed in both phases (Figure 11). Therefore, we may conclude that they are "passive" ions; i.e., they have no specific interactions with any of the other ions.

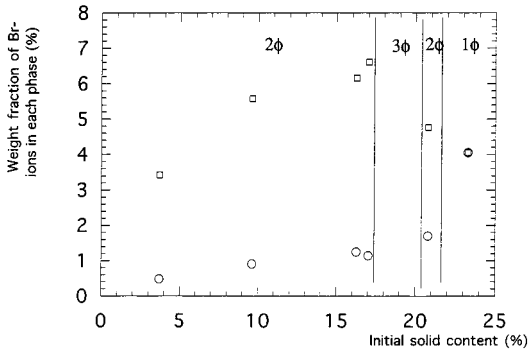

Figure 10. Weight fraction of Br^- ions in each phase versus the initial solid content.

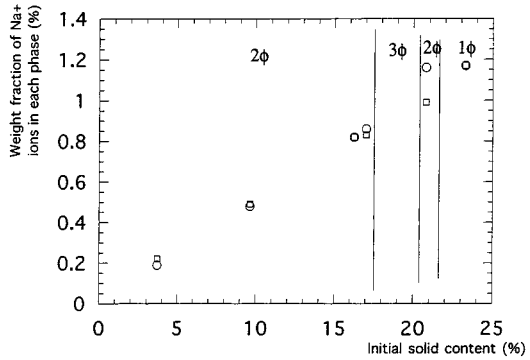

Figure 11. Weight fraction of Na^+ ions in each phase versus the initial solid content.

The values of the compositions are also presented in Table 1.

In summary, the four ionic species distribute differently among the separating phases. Therefore, the system must really be treated in terms of five components (including water).

Discussion

The central feature of the NaPA + CTABr system is the associative phase separation into one or two concentrated phase-(s) that contain most of the PA^- and CTA^+ ions and one dilute phase that contains most of the Na^+ and Br^- ions. We have observed that this separation occurs when water is added to a concentrated solution of NaPA and CTABr in water. We have also observed that the concentrated phase becomes still more concentrated as more water is added to the two-phase samples. In this section, we shall discuss this behavior in two steps. First, we shall examine how the structures of the concentrated phases are related to their compositions. Second, we shall try to explain why the phases separate in this way.

Structures and Compositions. All structures have been analyzed according to a model where the surfactant molecules form cylindrical aggregates, and these aggregates are packed on a hexagonal lattice. This is supported by Luzatti[15] who showed that when the CTABr weight fraction is higher than 0.1, the micelles are rodlike. As explained in the Results section, the variations in lattice parameters show that the surfactant molecules must be inside these cylinders. Conversely, the polyions must be in the water layers that separate the surfactant aggregates.

In this model, the lattice parameter a of the phase is obtained from the peak position q according to

$$a = \frac{2}{\sqrt{3}} \frac{2\pi}{q}$$

TABLE 1: Elemental Composition of the Samples and of the Separated Phases

Global Concentration

sample	NaPA (%)	CTABr (%)	water (%)
1	4.26	16.52	79.15
2	3.49	13.54	82.94
3	3.33	12.93	83.7
4	1.98	7.66	90.34
5	0.76	2.95	96.28

Dilute Phase

sample	Na^+ (%)	Br^- (%)	PA^- (%)	CTA^+ (%)	water (%)
1	1.16	1.70	2.43	1.41	93.30
2	0.86	1.14	1.67	0.00	96.33
3	0.82	1.25	1.41	0.00	96.51
4	0.48	0.91	0.70	0.00	97.91
5	0.19	0.48	0.14	0.00	99.19

Concentrated Phase

sample	Na^+ (%)	Br^- (%)	PA^- (%)	CTA^+ (%)	water (%)	COO/Br
1	0.99	4.76	3.78	19.70	70.77	0.89
2	0.83	6.61	4.65	31.59	56.31	0.79
3	0.82	6.16	4.94	31.31	56.78	0.90
4	0.49	5.58	5.70	36.38	51.84	1.15
5	0.22	3.42	7.67	39.78	48.92	2.53

TABLE 2: Cylinder Radii and Surface Areas per Surfactant Ion Headgroup

phases	initial solid content	weight fraction of CTA^+ in the concentrated phase	lattice parameter a (Å)	cylinder radius R (Å)	area/surfactant headgroup A (Å^2/molecule)
hexagonal	0.28	0.22	79.2[a]	19.5	48.5
phase of	0.61	0.476	54.1[a]	19.6	48.5
CTAB in	0.65	0.504	53.7[b]	20.06	47.2
water					
I_{conc}	0.209	0.174	85.3	18.7	50.6
E	0.2	0.316	62	18.3	51.6
E	0.044	0.398	51.8	17.5	55

[a] Reference 17. [b] Reference 16.

Then the radius R of the cylinder can be calculated from the lattice parameter and from the volume fraction ϕ of the surfactant ions in the phase as

$$R = a\sqrt{\frac{\phi\sqrt{3}}{2\pi}}$$

Finally, the surface area A per surfactant molecule at the micellar surface may be calculated from a, ϕ, the mass M of a surfactant ion (M = 284.6 g/mol), and its density ρ (=1 g/cm^3)

$$A = \frac{2M}{a\rho}\sqrt{\frac{2\pi}{\phi\sqrt{3}}}$$

We start this analysis with the phases of pure CTABr. In Table 2 (first three lines)[16,17] we present the solid content of each phase, the weight fraction ϕ of CTA^+ ions that make the cylindrical aggregates, and the calculated geometrical parameters of the structure: the lattice parameter a, the cylinder radius R, and the surface area per surfactant ion headgroup A. The radius R and the area A remain nearly constant, even though the volume fraction of the surfactant ions is changed by a factor of 3. Accordingly, when water is removed from the phase, the cylindrical aggregates remain the same; only their distances change. This was previously observed by Luzatti[18] in various surfactant hexagonal phases.

Then we consider the results from the mixtures of CTABr and NaPA. The data from the micellar phase I_{conc} and from the hexagonal phase E are presented in Table 2 (bottom three lines). In this case, when water is added to the system (initial solid content decreasing from 0.209 to 0.044), the weight fraction of CTA^+ ions in the concentrated phase increases (from 0.174 to 0.398). Contrary to the case of pure CTABr, the radius R decreases and the area A increases as the phase becomes more concentrated. Of course, the decrease of the cylinder radius and the increase in the headgroup area are related, since the cylinders are completely filled with the surfactant chains.

This structural variation of the surfactant aggregates must originate from the effects of the polyion. In the concentrated phases, the PA^- polyions replace the original Br^- counterions of the surfactant. A measure of this competition is given by the ratio of the COO^- group to the Br^- counterion in the concentrated phases. The results are presented in Table 1.

According to these values, the addition of a small amount of water to the mixture gives rise to the formation of a dilute phase, leaving behind a more concentrated I_{conc} phase that has a relatively low CTA^+ content (ϕ = 0.197) and where the charges of the macroions are still compensated mainly by Br^- counterions (COO^-/Br^- = 0.89). On the other hand, the addition of a large amount of water gives rise to the formation of an even more concentrated mesophase (E), which has a higher CTA^+ content (ϕ = 0.398) and where the charges of the surfactant macroions are compensated mainly by the COO^- groups of the PA^- polyions (COO^-/Br^- = 2.53).

Altogether, these results show a consistent trend where the addition of water pulls the Br^- ions into the dilute phase, and they are replaced in the concentrated phase by COO^- groups of the polyion. It is well-known that bromide ions are strongly condensed on the micellar surfaces,[19−21] whereas carboxylate ions are not. Therefore, the change in the surface area per molecule must result from the exchange of ions, where the polyion progressively displaces the bromide counterions of the surfactant.

The same results also show that the lattice parameter of the phase decreases when water is added to the two-phase samples. This variation can also result from the competition between the polyions and the bromide counterions of the surfactant. Indeed, at large additions of water, the polyions have displaced most of the bromide ions, and electrostatic attractions will force them to collapse on the oppositely charged surfaces of the surfactant macroions. Consequently, the repulsion between the surfactant cylinders decreases.

In summary, the variations of the structures of the concentrated phases result from the progressive displacement of the bromide counterions of the surfactant by the polyacrylate polyions. We must now examine how the various ions distribute among the phases to produce this displacement.

Phase Diagrams and Their Interpretation. The above analyses of the compositions of the separating phases have clearly shown that the stoichiometric mixtures cannot be described in terms of two salts only. Thus, representations of the phase diagram in terms of either the conventional mixing plane or the alternative mixing plane (cf. the Introduction) are both unsatisfactory. Thalberg et al.[13] resolved this problem by presenting their mixtures in pyramid-shaped phase diagrams, as shown in Figure 1. However, these diagrams, although appealing, have the disadvantage that they are difficult both to draw and to read.

We have chosen another alternative (Figure 12) by drawing diagrams that show the distributions of the *ions* in the separating

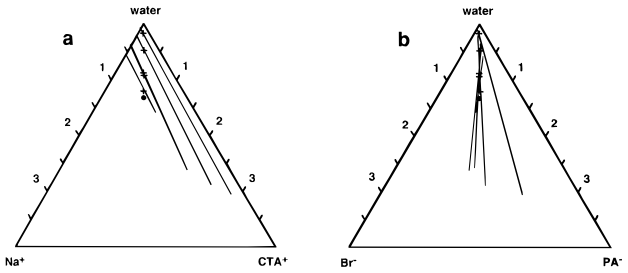

Figure 12. Phase diagrams showing the distributions of the cations (a) or the anions (b) between the separated phases. The overall compositions are indicated by crosses. The circles indicate one-phase samples.

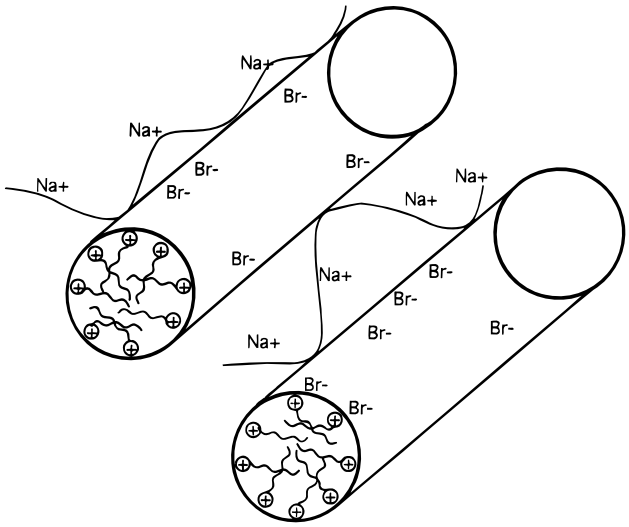

Figure 13. Schematic view of possible polyion configurations in the hexagonal phase.

phases. The diagrams in Figure 12 correspond to side views of the pyramid similar to that shown in Figure 13 of ref 13. The cations (Na^+ and CTA^+) are shown in Figure 12a and the anions (Br^- and PA^-) in Figure 12b. All concentrations are in moles of charge per kilogram of water. Since both phases contain, in general, all four ions, each axis represents the sum of two salts. (For example, the CTA^+ axis represents the sum of the concentrations of CTABr and CTAPA.) As usual, two phases in equilibrium with each other are connected by a tie-line, and the global composition of the mixture is indicated as a point on the tie-line. Since all investigated mixtures were stoichiometric, the global compositions all lie on the bisectors of the diagrams. The composition of the original monophasic mixture, close to the onset of phase separation, is also indicated in each diagram. When such a mixture is diluted with water (i.e., the global composition moves toward the water corner), the system separates into two phases, as we have seen previously, and the concentrated phase becomes increasingly concentrated as the degree of dilution is increased, in agreement with the predictions made in the Introduction.

Each diagram in Figure 12 shows the distributions of one monovalent ion (M) and one polyion (P) of the same charge. As a useful reference case, we consider first a perfectly symmetrical mixture (cf. Figure 2), where P^+ and P^- are identical in all respects except for the signs of their charges (+ or −), and the same holds for M^+ and M^-. For such a system, the two diagrams corresponding to parts a and b of Figure 12 would have to be identical for reasons of symmetry. For the same reason, as pointed out in the Introduction, all compositions of the separating phases must be describable in terms of the complex salt P^+P^-, the simple salt M^+M^+, and water. This is because the relations $[P^+] = [P^-]$ and $[M^+] = [M^-]$ must hold in a symmetrical system. In the real system, however, we see that there are large differences between the phase diagrams. This shows directly that the system is not describable only in terms of a mixture of the complex salt and the simple salt. We will argue below that this breaking of symmetry is due to two effects: differences between the polyions and contributions of chemical specificity in the interaction between CTA^+ and Br^-. [Note that if the phase compositions could have been described in terms of the three components CTABr, NaPA, and water only—the normal quasi-ternary representation—then the CTA^+ axis in Figure 12a would obviously have been equivalent to the Br^- axis in Figure 12b and similarly for the Na^+ and PA^- axes. The two diagrams would then have been mirror reflections of each other in the bisector representing the global compositions. Clearly, this is even further from the real situation.]

Figure 12a shows that, as already noted, the distribution of CTA^+ between the phases is extremely unequal; virtually all of the surfactant ions are in the concentrated phase, and the dilute phase only contains a small concentration of monomeric surfactant ions. After the hexagonal-to-isotropic transition, the CTA^+ concentration in the concentrated phase decreases quite significantly. All these features may be understood if we regard the aggregates in the hexagonal phase as stiff rods of effectively infinite length, while the micelles in the isotropic concentrated phase are of finite length.

The distribution of PA^- in Figure 12b shows considerably more variation when the total concentration of polyelectrolyte and surfactant is increased. At very low concentrations, the distribution of the polyion is similar to that for the surfactant ion; virtually all of the polyion is in the bottom phase. In fact, we expect the tie-lines for PA^- and CTA^+ to become increasingly similar and to move increasingly close to the water−polyion axes as the dilution approaches infinity. In this limit, both tie-lines reflect the phase separation between the hydrated, neutral complex salt and essentially pure water. As the overall concentration increases, however, the concentration of PA^- in the dilute phase increases rapidly. At the same time, the content of bromide in the concentrated phase increases at the expense of the PA^- concentration. Thus, as the total concentration increases, bromide replaces polyacrylate in the concentrated phase and more and more polyacrylate goes to the dilute phase. Two mechanisms should contribute to this effect. The first is that the polyion, being much smaller and flexible, is intrinsically much more soluble than the surfactant aggregate. Phrased alternatively, the entropic cost of confining all polyions to the concentrated phase is much larger for PA^- than for aggregates of CTA^+. Moreover, bromide is known to bind preferentially (over ions such as chloride) to cationic surfactant ions. There is thus an element of chemical competition to the binding sites. As the salt concentration becomes higher, the intrinsically higher affinity of the bromide ion to the binding sites becomes more and more important. At very low concentrations, on the other hand, entropy governs the systems, and in this limit, the valency alone (the multivalent PA^- versus the monovalent Br^-) determines the preferential binding.

Finally, we turn back to Figure 12a and look at the partitioning of the sodium ion. We see there that the sodium concentration, in molal units, is actually larger in the concentrated phase than in the dilute phase. (This feature was not evident in Figure 11 above because there the concentrations were expressed as the mass fractions of each phase.) This means that the Na^+/H_2O ratio is larger in the concentrated phase and

remains so even when the global concentration increases. This is not at all obvious. It means that we cannot describe the concentrated phase simply as a mixture of two types of surfactant salts, CTABr and CTAPA, where the bromide counterions increasingly replace the PA^- ions, which are released into the large dilute phase. There is in addition an increasing excess concentration of small sodium (and, consequently, bromide) ions in the concentrated phase. The enrichment of simple salt (NaBr) in the concentrated phase is entropically unfavorable and can only be due to a binding of sodium ions to PA^- in the bottom phase. Expressed alternatively, all the charges of a PA^- ion are not neutralized by surfactant ions; some are neutralized by sodium ions. Two effects may contribute to this. First is the chemical affinity of the Br^- for the CTA^+ surfaces, which makes it difficult for COO^- to displace Br^-. Second, configurational entropy of the flexible polyacrylate ion is gained if it is allowed to partially come off the surface of the surfactant macroion in loops and tails. These loops and tails must then be neutralized by small counterions. The situation, illustrated in Figure 13, is much like that of the adsorption of a flexible polyion to an oppositely charged surface in the presence of excess salt. The fraction of adsorbed segments of the polyion decreases gradually as the salt concentration increases. The extension of the adsorbed polyion further and further into the surrounding solution contributes to the swelling of the concentrated phase.

Conclusions

Aqueous mixtures of polyelectrolytes and oppositely charged surfactants tend to separate in ways that appear, at first, surprising. Indeed, addition of water causes phase separation and an addition of salt resolubilization. Moreover, the structural evolution of the concentrated phase is also unusual: addition of water causes it to deswell.

These processes are surprising only if the system is described as a ternary system made of water, surfactant, and polyelectrolyte. Following Kyrre Thalberg, we have recognized that the system actually contains water and four ionic species: the surfactant ion, its bromide counterion, the polyion, and its sodium counterion. In the phase-separation process, these ions are partitioned in a way that does not reflect their origin (the added polyelectrolyte and the surfactant salts).

We have analyzed the structures and the ionic compositions of separating phases in stoichiometric mixtures of sodium polyacrylate and cetyltrimethylammonium bromide. The result can be described as an ion-exchange process, where the PA^- polyions displace some Br^- counterions of the surfactant ions. Systems that contain a large amount of water can then gain entropy by releasing simple ions (Na^+ and Br^-) into a dilute aqueous phase, while the surfactant ions and the polyions form a concentrated micellar phase or a mesophase. Systems that contain less water do not undergo a complete ion exchange. The concentrated phase then swells because the polyions are progressively desorbed from the surfaces of the surfactant macroions by the Br^- ions, and at high concentrations both phases merge.

We propose to represent these ion exchanges by drawing two diagrams that represent the distribution of ions in the separating phases. One diagram describes the competition of anions: displacement of the Br^- counterions of the surfactant aggregates by the PA^- polyions. The other one describes the competition of cations: displacement of the Na^+ counterions of the polyelectrolyte when the PA^- polyions collapse on the surfactant aggregates. This representation makes it possible to characterize immediately the type of phase separation occurring in a particular system. For the reference case where the pure complex salt (CTA^+PA^-) separates from simple salt (Na^+Br^-), both diagrams should be identical. For real cases, differences between both diagrams reveal the differences between the polyions and surfactant ions, as well as the chemical specificity of interaction between CTA^+ and Br^-. Moreover, this is a rigorous representation of the five-component system.

Finally, we would like to point out that many of the conclusions in this paper, as well as the strategies in elucidating the phase behavior (i.e., the use of stoichiometric mixtures and dilution with water as a means to generate separating phases, the analysis of the results in terms of the two possible mixing planes), are relevant not only for oppositely charged polyelectrolyte/surfactant mixtures but also quite generally for systems that are, or may be described as, mixtures of two oppositely charged polyelectrolytes.

Acknowledgment. P. Lixon is gratefully acknowledged for her help in the analyses. This work was partially funded by Rhône-Poulenc. L.P. acknowledges funding from the Swedish Research Council for Engineering Sciences (TFR). B.C. and L.P. acknowledge travel funds from the EU Human Capital and Mobility program (Contract No. CHRX-CT94-0655, "Water Soluble Polymers").

References and Notes

(1) Thalberg, K.; Lindman, B. *Interactions of Surfactants with Polymers and Proteins*; Goddard, E. D., Ananthapadmanabhan, K. P., Eds.; CRC Press: Bocca Raton, FL, 1993; pp 203−276.
(2) Piculell, L.; Lindman, B. *Adv. Colloid Interface Sci.* **1992,** *41*, 149−178
(3) Carnali, J. O. *Langmuir* **1993**, *9*, 2933−2941.
(4) Antonietti, M.; Wenzel, A.; Thünemann, A. *Langmuir* **1996**, *12*, 2111−2114.
(5) Antonietti, M.; Kaul, A.; Thünemann, A. *Langmuir* **1995**, *11*, 2633.
(6) Antonietti, M.; Conrad, J.; Thünemann, A. *Macromolecules* **1994**, *27*, 6007−6011
(7) Masa-aki, Wakita; Edwards, K. A.; Regen, S.; Turner, Dand; Gruner, M. S. *J. Am. Chem. Soc.* **1988**, *110*, 5221.
(8) Everaars, D. M.; Nieuwkerk, C. A.; Denis, S.; Marcelis, T. M. A.; Sudhölter, E. J. R. *Langmuir* **1996**, *12*, 4042.
(9) Thalberg, K.; Lindman, B. *Surfactants in solution*; Mittal, K. L., Shah, D. O., Eds.; Plenum Press: New York, 1991.
(10) Thalberg, K.; Lindman, B.; Karlström, G. *J. Phys. Chem.* **1991**, *95*, 3370.
(11) Thalberg, K.; Lindman, B.; Karlström, G. *J. Phys. Chem.* **1990**, *94*, 4289.
(12) Thalberg, K.; Lindman, B.; Bergfeldt, K. *Langmuir* **1991**, *7*, 2893.
(13) Thalberg, K.; Lindman, B.; Karlström, G. *J. Phys. Chem.* **1991**, *95*, 6004.
(14) Ranganathan, S.; Kwak, J. C. T. *Langmuir* **1996**, *12*, 1381−1390.
(15) Reiss-husson, F.; Luzzati, V. *J. Phys. Chem.* **1964**, *68*, 3504.
(16) Ekwall, P.; Mandell, L.; Fontell, K. *J. Colloid Interface Sci.* **1969**, *29*, 639.
(17) Vethamuthu, M. S.; Almgren, M.; Bergenstahl, B.; Mukhtar, E. *J. Colloid Interface Sci.* **1996**, *178*, 538.
(18) Reiss-Husson, F.; Mustacchi, H.; Luzzati, V. *Acta Crystallogr.* **1960**, *13*, 668.
(19) Auvray, X.; Petipas, C.; Anthore, R.; Rico, I.; Lattes, A. *J. Phys. Chem.* **1989**, *93*, 7458.
(20) Toullec, J.; Couderc, S. *Langmuir* **1997**, *13*, 1918.
(21) Thalody, B.; Warr, G. G. *J. Colloid Interface Sci*., in press.